Experimental and theoretical investigation of BCl_3 decomposition in H_2

Guillaume Reinisch, Jean-Marc Leyssale, Nathalie Bertrand, Georges Chollon, Francis Langlais, Gerard L. Vignoles

Experimental and theoretical investigation of BCl_3 decomposition in H_2

G. Reinisch[a,*], J.-M. Leyssale[a], N. Bertrand[b], G. Chollon[a], F. Langlais[a], G. Vignoles[b]

a) CNRS, Laboratoire des Composites ThermoStructuraux, UMR 5801 CNRS-CEA-Snecma Propulsion Solide-UB1, 3 allée de La Boétie, 33600 Pessac, France
b) Univ. Bordeaux 1, Laboratoire des Composites ThermoStructuraux, UMR 5801 CNRS-CEA-Snecma Propulsion Solide-UB1, 3 allée de La Boétie, 33600 Pessac, France

Abstract

A combined experimental and theoretical study of the homogeneous decomposition of BCl_3 in a H_2 carrier gas is presented. A detailed description of the B/Cl/H thermodynamic equilibrium is first obtained from ab initio calculations from which a restricted low energy chemical mechanism is identified to model the decomposition of BCl_3. Transition state theory is then invoked to obtain reaction rates and the resulting kinetic mechanism is incorporated in a 1D model of a CVD reactor. Comparison of calculated steady state concentrations with in situ FT-IR measurements shows a good agreement at low temperatures, thus validating the kinetic model. The divergence observed at higher temperatures is attributed to boron deposition.

Key words : Chemical Vapor Deposition, Boron, Boron Carbide, Ab-initio computation, Chemical Kinetics.

* To whom correspondence should be addressed : reinisch@lcts.u-bordeaux1.fr

Introduction:

Self-healing Ceramic-Matrix Composites (CMCs) are promising materials for demanding aeronautic applications, *i.e.* simultaneous exposition to heat, mechanical loads, and oxidizing atmospheres. Their internal protection against oxidation can be based on boron-containing matrix layers, because of their ability to generate a liquid oxide, which acts as a diffusion barrier [1]. Accordingly, the preparation of these materials relies on the precise control of the boron-containing layer thicknesses. Chemical Vapor Deposition (CVD) is the privileged method for their production, since it allows, by a precise tuning of the reaction to diffusion ratio, to achieve deposit uniformity inside a complex fibrous medium. In that case the process is termed CVI (Chemical Vapor Infiltration) and operates usually at low pressures and moderate temperatures.

As boron hydrides like BH_3 are extremely toxic and hazardous, boron halides and in particular BCl_3 are commonly used as boron precursors. The decomposition of BCl_3 in a hydrogen-rich CVD reactor is however not fully characterized. Most experimental papers [2-5] report only on deposition rates, while little or no information is given on the gas phase decomposition of BCl_3. Nonetheless, Sezgi *et al.* [2] indicate that $BHCl_2$ is the main gaseous product in atmospheric pressure CVD. Several modeling works have been performed in parallel to these experimental characterizations; featuring separately or together: thermochemical equilibrium computations, mass-transfer modeling, and chemical kinetic mechanisms. Two gas phase mechanisms, based on *ab-initio* calculations, have been proposed. Harris *et al.* [6] proposed a mechanism based on 31 chemical reactions. The decomposition of BCl_3 starts with the reaction $BCl_3+H\rightarrow BCl_2+HCl$, which depends itself on a first H_2 dissociation step. No direct validation with experimental data has been given.

More recently, in the frame of a B-doped Si CVD modeling study, Lengyel and Jensen have proposed a restricted mechanism [7], which takes only into account the three bimolecular reactions listed later in table 2. None of these reactions were involved in the previous mechanism [6]. No direct validation with respect to gas-phase experimental data has been given; however the boron mass uptake data have been reproduced using fitted sticking coefficients. Accordingly, there are still some open questions concerning the decomposition of BCl_3 in H_2, especially at low pressures; this has motivated the present study. Here, the emphasis is set on the gas phase characterization and modeling, from *ab-initio* methods to reactor simulation.

Experimental:

Decomposition experiments are performed in a low pressure hot wall tubular reactor. A mixture of BCl_3 and H_2 flows through a vertical silica tube heated by a graphite susceptor coupled to a radio-frequency inductive coil. The tube section is 34 *mm* in diameter and the hot isothermal zone length is 140 *mm*. The reactor outlet is connected to an FT-IR spectrometer for a quasi in-situ chemical analysis using transmission mode: the gases are thus analyzed after cooling down to ambient temperature.

The operating conditions are typical of the CVI process [8]: (i) pressure between 1 and 10 *kPa*, (ii) temperature between 800 and 1300 *K*, (iii) total flow rate 100 to 500 *sccm* (std. cm^3 per second), (iv) initial dilution ratio $[BCl_3]/[H_2]$ = 1/2 to 1/10. At each parameter set, data were collected at different times to check that a steady state is reached. Two independent mechanisms for relaxation towards steady state were identified: first, gaseous chemical equilibrium is reached a few minutes after the start of experiment; then, reactor thermal and mechanical steady-state achievement may take up to 20 minutes, and depends on the chosen temperature program. Not taking this last point into account may be a large source of error.

Numerical methods:

The modeling strategy starts with quantum chemical computations. First, equilibrium geometries, harmonic vibration frequencies and potential energy surfaces of a large set of chemical species in the system B/Cl/H are computed under the Density Functional Theory (DFT) framework at the B3Lyp/6-31G(d,p) level of theory using the Gaussian 2003 package [9]. This set includes H_2, HCl, Cl_2 and BH_iCl_j ($0 \leq i+j \leq 4$) species.

Vibration frequencies, known for being overestimated by DFT calculations, are scaled by the usual factor of 0.96. Partition functions, entropies and heat capacities are obtained from the well-known statistical equations [10].

Central to the prediction of reaction rate constants is the calculation of the activation energy of the reaction, namely the potential energy difference between the transition state and the reactants (*e.g.* a variation of a few *kcal/mol* in the activation energy can change a reaction rate by several orders of magnitude). Calculation of energies thus requires numerical methods of high accuracy. In this work, we use the G3B3 method [11], in which the energy is obtained from single point calculations (at the equilibrium B3Lyp/6-31G(d) geometry) at four different levels of theory (QCISD(T,E4T)/6-31G(d), MP4/6-31+G(d), MP4/6-31G(2df,p), MP2=Full/GTLarge), taking into account the electronic correlation to a large extent and a spin-orbit correction. Calculation with this method of $\Delta H_f^0(298K)$ of 155 molecules has given a root mean square deviation of only 1.37 kcal/mol [12].

Thermochemical computations:

The obtained heats of formations for all the investigated compounds are presented table 1. Such a calculation requires the knowledge of atomic heats of formation. We use the values from JANAF tables [13] for chlorine (28.98 kcal/mol) and hydrogen (52.07 kcal/mol) and the value recommended by Gurvich *et al.* [14] (134.93 kcal/mol) for boron. Experimental values (from [13] and [14]) are given for comparison; the average standard deviation of the com-

puted values with respect to these data shows that the agreement is excellent, especially with the Gurvich data. Discrepancies with JANAF tables concern primarily BH_2, BCl_2 and BCl, most probably due to inaccuracies in these tables; indeed, similar computational results obtained with other high level quantum chemistry methods [12, 15, 16] are coherent with our values.

Thermodynamic equilibria and for an initial composition ratio of $[H2]/[BCl_3]=5$ are presented on figure 1 (molecular species) and figure 2 (radicals species). It is obvious from these figures that the gas, at low temperature, is almost only composed of molecules (mainly H_2, HCl, BCl_3, $BHCl_2$) and that radicals start to appear at temperatures larger than 1500K, BCl being the preponderant one.

In order to test the possibility of dimerization or homogeneous nucleation, we included some diborane species (B_2X_i X=Cl, H, i=4, 5, 6; $B_2H_jCl_4$ j=0, 1, 2) and boron clusters (B_kX_k X=H, Cl, k=9,12; and $B_{12}H_6Cl_6$) in our model. We observed that all these species are in negligible quantities whatever the temperature.

Kinetic mechanism:

The determination of a kinetic mechanism first requires the calculation of the energy barriers associated to the chemical reactions which can take place in the gas phase. Looking at the typical CVD or CVI processing conditions, for $T < 1500\ K$, we have concluded from the thermodynamic study that only a few light molecular species occur. As a consequence the reactions listed in table 2 are the most important candidates for the low temperature mechanism, furthermore considering that the energy barriers for their conversion are moderate (about 40 *kcal/mol* [7]).

We have thus reexamined Lengyel's mechanism [7] at the G3B3 level of theory (in their original work the DFT B3LYP/6-31G(2d,p) level was used). Transition states, energy barriers and partition functions have been characterized and the corresponding rate constants ap-

proximated, according to Transition State Theory (TST). These reaction rates are fitted to an Arrhenius law; activation energies and pre-exponential factors are shown in table 2.

CVD reactor model :

The experimental reactor was first modeled to characterize the temperature profile along its axis. Total mass, momentum, and energy equations (featuring radiative heat transfer) were solved using a finite-volume software.

Figure 3 shows a typical temperature field obtained with 200 *sccm* of pure H_2 at 1 *kPa* and a susceptor temperature of 1300K. The radial temperature gradient is low and a one-dimensional simulation represents a good approximation. Doubling the mass flow rate did not have a large influence: only a 2 *mm* lag on the axial temperature profile has been obtained. Also, composition did not have a large influence at high dilution because in every case H_2 is mainly responsible for heat conduction. For susceptor temperatures different from 1300 *K* it has been sufficient to consider a scaled profile based on the normalized 1300 *K* result. Once the temperature distribution is known, the species mass balance equations are solved using 1D-model and in steady state.

Results:

Figure 4 presents the steady state concentration of BCl_3, $BHCl_2$, HCl, BH_2Cl and BH_3 at the reactor outlet obtained by the 1D model implementing our new kinetic mechanism. We see on Figure 4 that BCl_3 starts to decompose in a pronounced manner when the temperature exceeds 750 *K*. The main products of this decomposition are $BHCl_2$ and HCl. Around 800 *K*, BH_2Cl starts to be observed in a non negligible amount. However, the ratio between BH_2Cl and $BHCl_2$ concentrations remains around 1/100 for temperatures between 800 and 1400 *K*. BH_3 can only be observed at extremely low concentrations. It is hard to say whether the observed concentrations of BH_3 are real or due to numerical inaccuracy. Also displayed on Figure 5 are the concentrations of BCl_3 and $BHCl_2$ when only the first reaction of the kinetic

mechanism ($BCl_3 + H_2$ -> $BHCl_2$ +HCl) is taken into account. We see that these concentrations are almost unaffected by the suppression of the two other reactions and that this single reaction is almost sufficient to properly describe BCl_3 decomposition in the investigated temperature range.

Let us now compare the results obtained with the new mechanism to our experimental data, to results obtained by the mechanisms of Harris et al. [6] and Lengyel et al. [7] and to the thermodynamic equilibrium situation. We were not able to detect experimentally the presence of BH_2Cl, which is coherent with Figure 4, showing that its concentration never exceeds 0.04 mol/cm^3. Results for BCl_3 and $BHCl_2$ are presented in figures 5 and 6 respectively. Experimental concentrations of BCl_3 and $BHCl_2$ are related to the IR signals with the hypothesis of complete transformation of BCl_3 in $BHCl_2$. It is seen first that the experimental decomposition of BCl_3 around 750 *K* coincides with the apparition of $BHCl_2$ situated between 600 and 800 *K* (the lowest temperature at which we observed $BHCl_2$ is 773 *K*). We also see on those figures that around 1000 *K* both BCl_3 and $BHCl_2$ concentrations are decreasing with temperature. As we do not observe any additional IR signal we attribute this loss of boron to the beginning of the boron deposition process, in agreement with the observations of Sezgi *et.al.* [2]. Comparing concentrations obtained with our new model to experimental measurements for temperatures below the deposition limit, we see that the model agrees qualitatively well with experiments but that a shift of roughly 80 *K* is observed (the concentration given by the model at *T* equals the experimental concentration at (*T*-80) *K*). Of course our model does not predict the deposition process at higher temperatures as it is a purely homogeneous model. When the model of Lengyel et al [7] is used, similar trends can be observed but in that case the shift with experiments is around 180 *K*. This shows that increasing the quality of the *ab-initio* description permits to reduce the gap between experiments and calculations.

When the model by Harris et al. [6] is used, we see from figure 5 (respectively figure 6) that the decomposition of BCl_3 (respectively the apparition of $BHCl_2$) starts around 1200 *K*, that is, more than 400 *K* hotter than the experimental observations. Such a discrepancy can only be attributed to a mechanism which does not take into account the chemistry responsible for the decomposition of BCl_3.

Concluding remarks:

CVD from BCl_3 and H_2 as precursors involves only three homogeneous molecular reactions at moderate temperature (T<1500K). Because of the relatively high activation energies of the radical initiation, the radical-containing route is negligible. Transition state theory was invoked at the G3B3 high level of theory to obtain reaction rates, and the resulting kinetic mechanism incorporated in a 1D model of our CVD reactor.

Theoretical steady state concentrations at the outlet of reactor agree well with experimental FTIR data at low temperature ($T < 1000$ *K*); the calculated values overestimate by only 80 *K* the evolution of the gas phase decomposition. This shift is about 180 *K* when using the mechanism of Lengyel *et al.* [7], which considers the same reaction but with data obtained at the lower DFT B3Lyp level of theory. Results obtained from the mechanism of Harris *et al.* [6] dramatically differ from experimental data because it does not take into account the molecular reactions.

At higher temperatures both BCl_3 and $BHCl_2$ steady state concentrations are overestimated by our model. This is linked to an experimental loss of homogeneous boron species, which agrees well with the start of deposition process at about 1000 *K*.

This work is the starting point for a broader study concerning the deposition of boron-containing carbides. It has been demonstrated here that the methodology is sound, as shown by the experimental validation; there remains to extend it to a larger gas-phase mechanism featuring carbon-containing species – for which validated kinetic databases already exist [17-

19] – and to complete it with heterogeneous kinetic data, obtained either by fitting experimental deposition results to gas-phase concentrations, as in [20], or by quantum dynamic studies.

Acknowledgements:

The Gaussian03 computations have been carried out at the M3PEC massively parallel computing facility of University Bordeaux 1. G. Reinisch acknowledges Snecma Propulsion Solide (Safran group) for PhD funding and wishes to thank R. Méreau (LPCM, University Bordeaux 1), C. Descamps (Snecma Propulsion Solide) for helpful discussions and S. Léger for help in CFD computations.

References :

[1]: R. Naslain, A. Guette, F. Rebillat, R. Pailler, F. Langlais and X. Bourrat, Journal of Solid State Chemistry 177 (2004) 449

[2]: N. A. Sezgi, T. Dogu, H. O. Ozbelge, Chemical Engineering Science 54 (1999) 3297

[3]: L. Vandenbulcke, G. Vuillard, J. Electrochem. Soc. 123, Issue 2, (1976) 278

[4]: L. Vandenbulcke, G. Vuillard, J. Electrochem. Soc. 124, Issue 12, (1977) 1931

[5]: T. Sekine, N. Nakanishi, E. Kato, J. Jpn. Inst. Met., 53 (1989) 698

[6]: S. J. Harris, J. Kiefer, Q. Zhang, A. Schoene, K.-W. Lee, J. Electrochem. Soc. 145 (1998) 3203.

[7]: I. Lengyel, K. F. Jensen, Thin Solid Films 365 (2000) 231.

[8]: J. Berjonneau, G. Chollon, F. Langlais, J. Electrochem. Soc. 153, Issue 12, (2006) 795

[9]: M. J. Frisch et al., Gaussian 03, Revision C.02 (2004), Gaussian, Inc., Wallingford, CT.

[10]: K. F. Jensen, Introduction to Computational Chemistry, 2nd ed. (Wiley, 2007).

[11]: L. A. Curtiss, K. Raghavachari, P. C. Redfern, V. Rassolov, J. A. Pople, J. Chem. Phys. 109 (1998) 7764.

[12]: B. Anantharaman, C. F. Melius, J. Phys. Chem. A 109 (2005) 1734.

[13]: M. W. Chase, C. A. Davies, J. R. Downey, D. J. Frurip, R. A. McDonald, A. N. Szverud, JANAF Thermodynamic Tables, 3rd ed., J. Phys. Chem. Ref. Data 14 (1985) 1985.

[14]: L. V. Gurvich, I. V. Veyts, C. B. Alcock, Thermodynamic Properties of Individual Substances, volume 3 (CRC Press: Boca Raton, 1994).

[15]: H. B. Schlegel, S. J. Harris, J. Phys. Chem. 98 (1994) 11178.

[16]: M. D. Allendorf, C. F. Melius, J. Phys. Chem. A 101 (1997) 2670.

[17]: J.C. Leylegian, H.Wang. Combustion and Flame, 114 (1998) 285.

[18] P.H. Taylor, D.A. Tirey, B. Dellinger, Combust. Flame 104 (1996) 260–271.

[19] P.H. Taylor, D.A. Tirey, B. Dellinger, Combust. Flame 105 (1996) 486–498.

[20]: C. Descamps, G. L. Vignoles, O. Féron, F. Langlais and J. Lavenac, J. Electrochem. Soc. 148 (2001) C695

Table 1: Room temperature heats of formation $\Delta_f H^{298K}$ (*kcal/mol*) of BCl_iH_j ($1 \leq i+j \leq 3$) calculated at the G3B3 level of theory together with experimental values taken from JANAF tables[a] [13] and from Gurvich et al.[b] [14] (available errors are given between parentheses). Absolute difference between theoretical and experimental value are indicated in Δ columns (*kcal/mol*).

$\Delta_f H^{298K}$	G3B3	Experiments[a]		Experiments[b]	
		Values	|Δ|	Values	|Δ|
BCl_3	-97.58	-96.3(0.5)	1.28	-96. 68(0.31)	0.9
$BHCl_2$	-60.36	-59.3(1)	1.06	-60.2	0.16
BH_2Cl	-19.6			-19.3(4.8)	0.3
BH_3	23.17	25.5(2.4)	2.33	21(2.4)	2.17
BCl_2	-7.55	-19(3)	11.45		
BClH	32.59	27.5	5.09	31(5)	1.59
BH_2	76.19	48(15)	28.19	76.1(2.6)	0.09
BCl	41.58	33.8(4)	7.78	41(6)	0.58
BH	103.48	105.8(2)	2.32	106.6(1.7)	3.12
|Δ| Average		7.44		1.11	

Table 2: Activation energy E_a (*kcal*/*mol*) and pre-exponential factor A (10^{13} cm^3/*mol*/*s*) for reactions (1-3). Values from Lengyel *et al.* [7] are indicated in parentheses for comparison.

	E_a	A
(1) $BCl_3+H_2 \rightarrow BHCl_2+HCl$	42.4 (43.2)	**6.06** (0.981)
(2) $BHCl_2+H_2 \rightarrow BH_2Cl+HCl$	38. (38.4)	2.39 (0.886)
(3) $BH_2Cl+H_2 \rightarrow BH_3+HCl$	30.5 (31.3)	2.80 (1.74)

List of figure captions

Figure 1: Equilibrium molar fractions of molecular species in the gas phase as a function of temperature.

Figure 2 : Equilibrium molar fractions of radicals in the gas phase as a function of temperature.

Figure 3: Temperature field obtained with 200 *sccm* pure H_2 at 1 *kPa* and a susceptor temperature of 1300 *K*.

Figure 4: Steady state concentrations at the reactor outlet as a function of temperature obtained from a 1D model of a CVD furnace using our new kinetic mechanism, either with a 3-reaction model (lines), or with a 1-reaction model (symbols).

Figure 5: Steady state BCl_3 concentration at the reactor outlet as a function of the susceptor temperature.

Figure 6: Steady state $BHCl_2$ concentration at the reactor outlet as a function of the susceptor temperature.

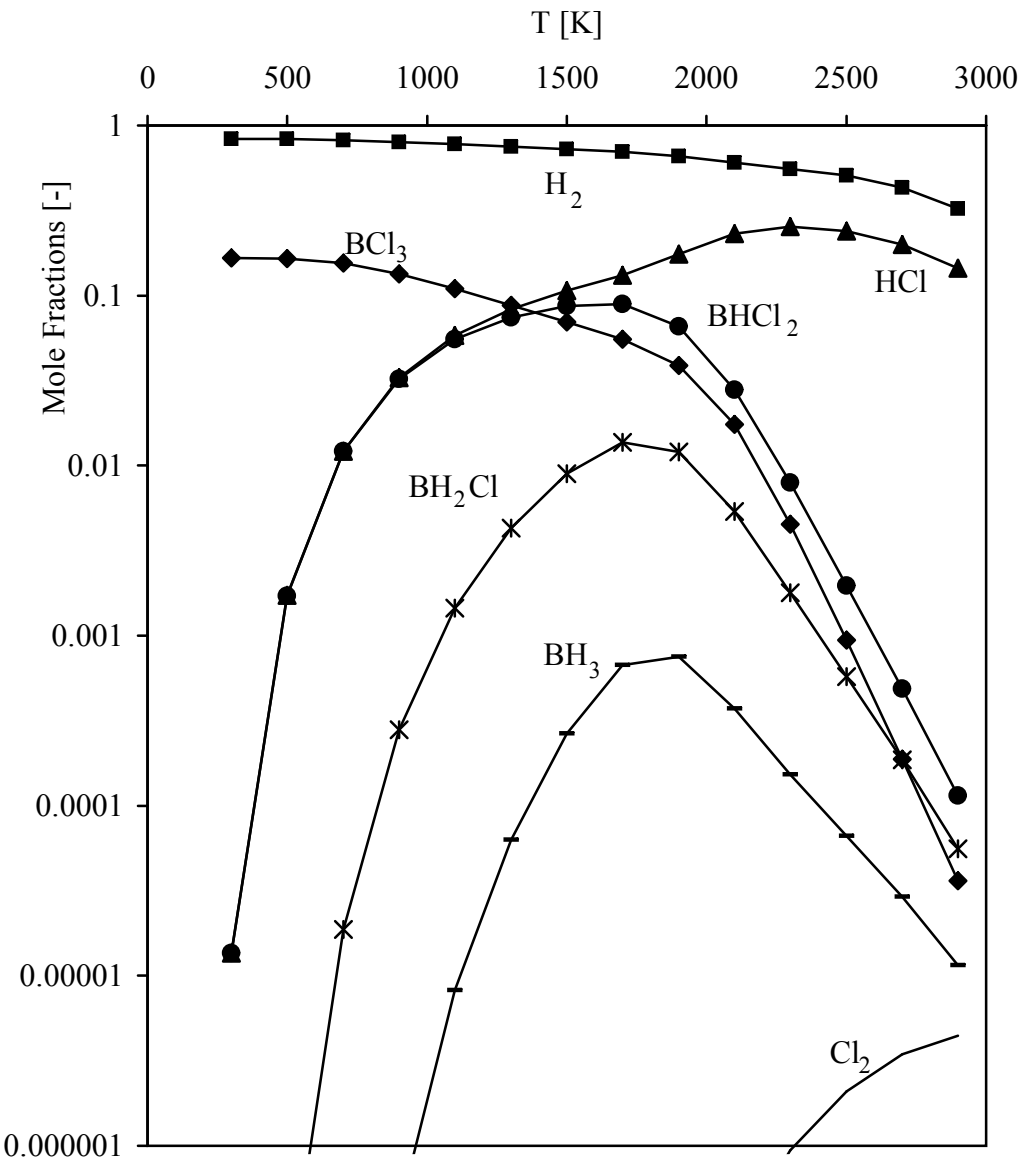
T [K]
0
500
1000
1500
2000
2500
3000
1
0.1
0.01
0.001
0.0001
0.00001
0.000001
Mole Fractions [-]
H2
BCl3
HCl
BHCl2
BH2Cl
BH3
Cl2

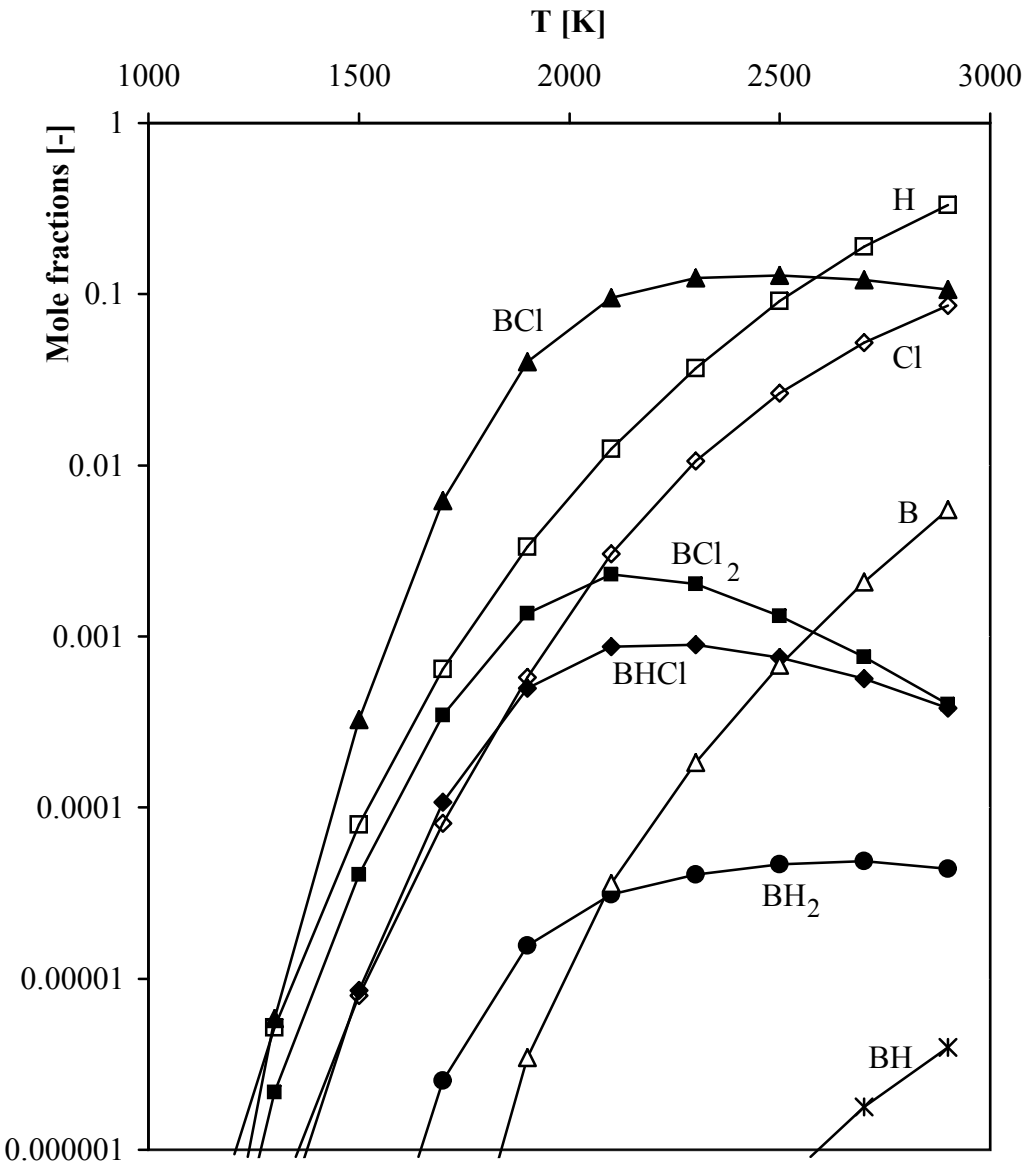
T [K]
1000
1500
2000
2500
3000
Mole fractions [-]
1
0.1
0.01
0.001
0.0001
0.00001
0.000001
H
BCl
Cl
B
BCl2
BHCl
BH2
BH

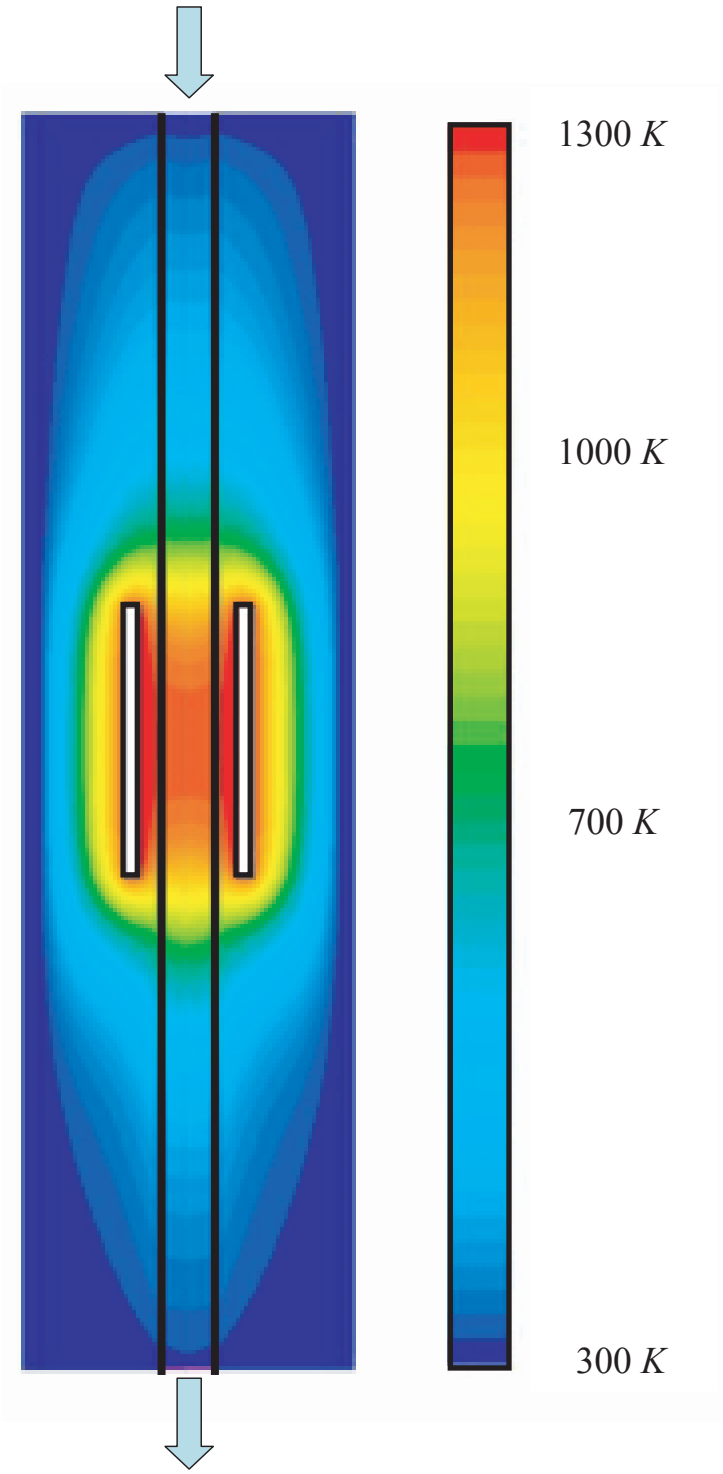
1300 K
1000 K
700 K
300 K

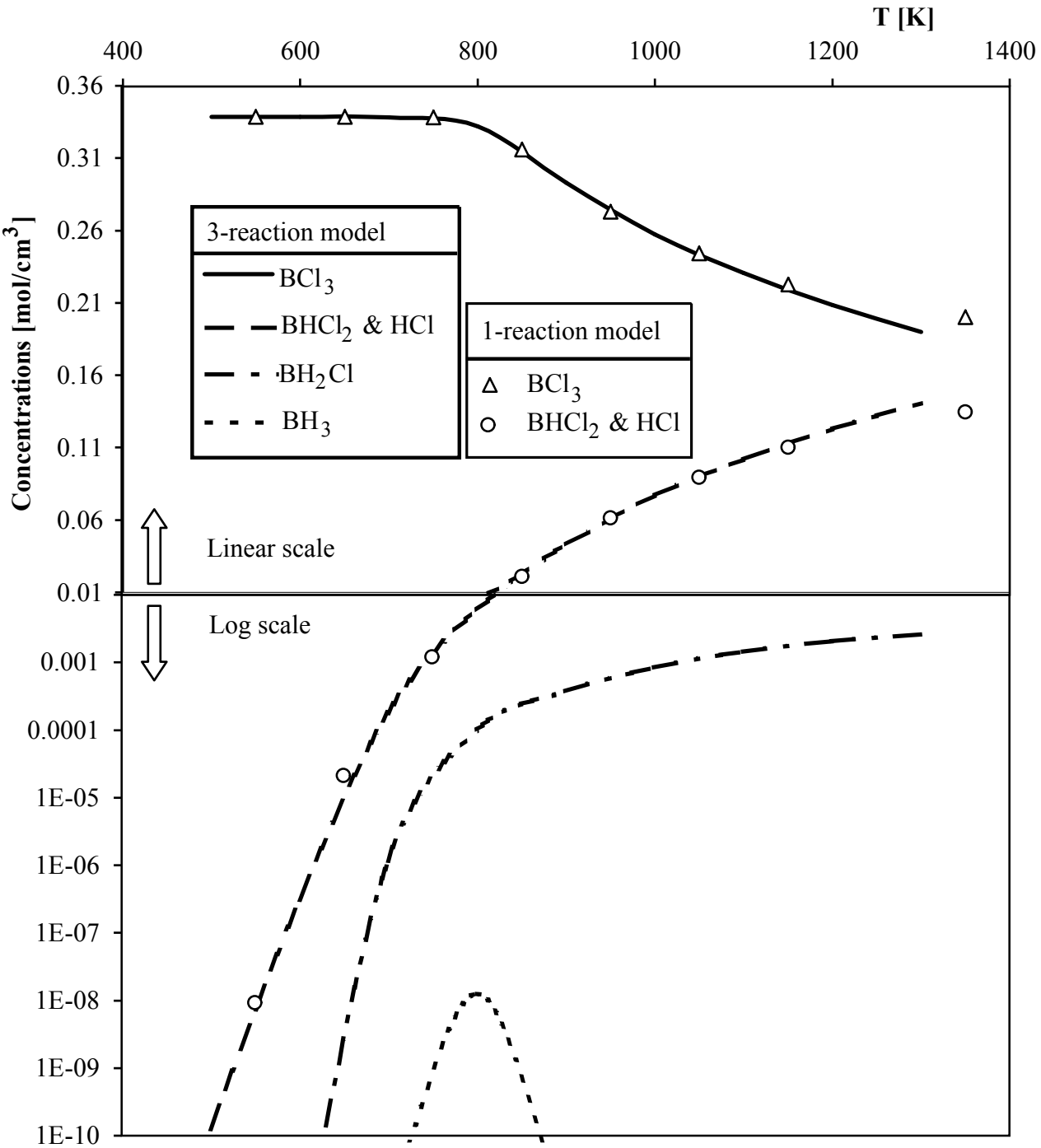
T [K]
400
600
800
1000
1200
1400
0.36
0.31
0.26
0.21
0.16
0.11
0.06
0.01
0.001
0.0001
1E-05
1E-06
1E-07
1E-08
1E-09
1E-10
Concentrations [mol/cm3]
3-reaction model
BCl3
BHCl2 & HCl
BH2Cl
BH3
1-reaction model
BCl3
BHCl2 & HCl
Linear scale
Log scale

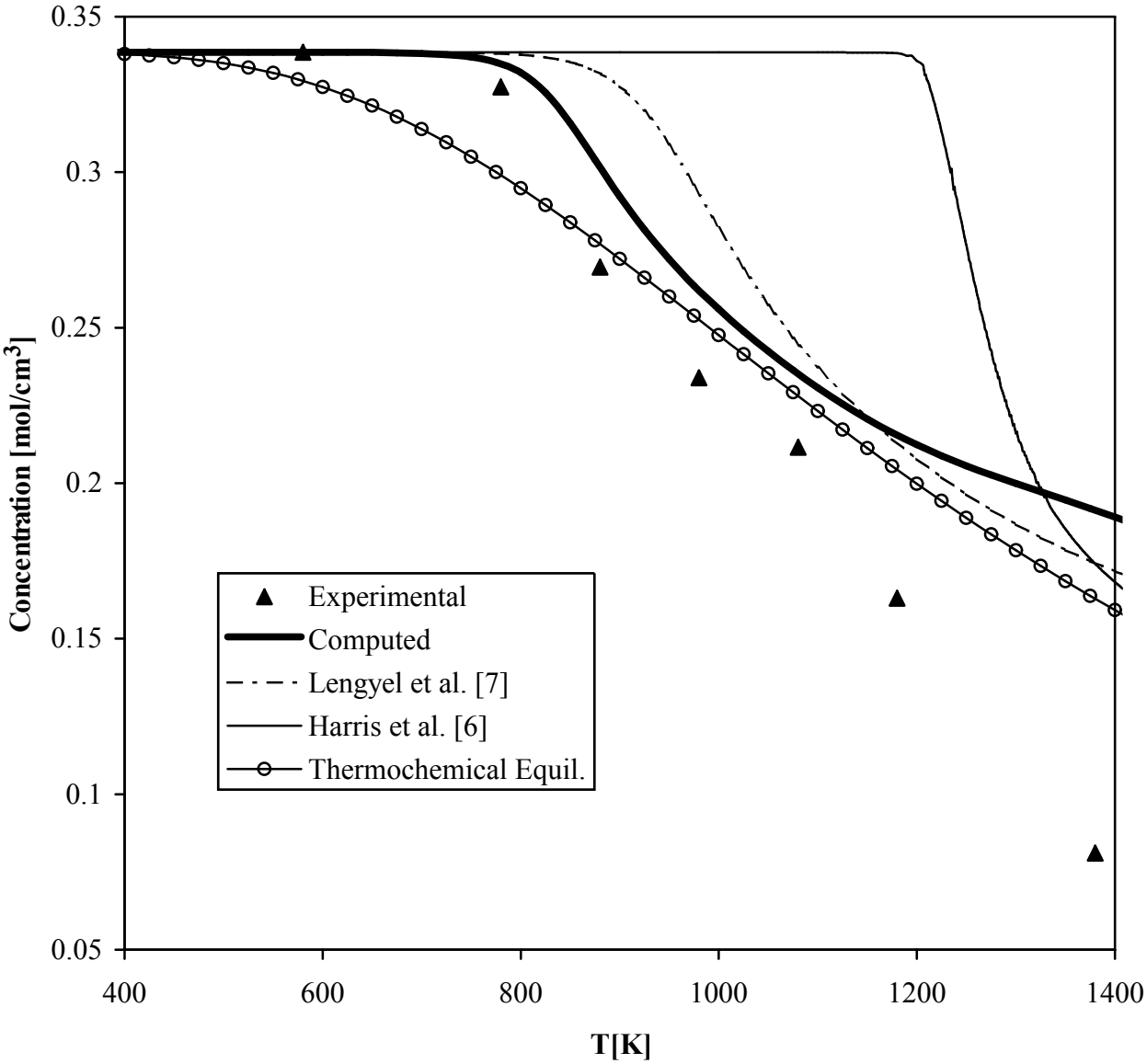
0.35
0.3
0.25
0.2
0.15
0.1
0.05
Concentration [mol/cm3]
400
600
800
1000
1200
1400
T[K]
Experimental
Computed
Lengyel et al. [7]
Harris et al. [6]
Thermochemical Equil.

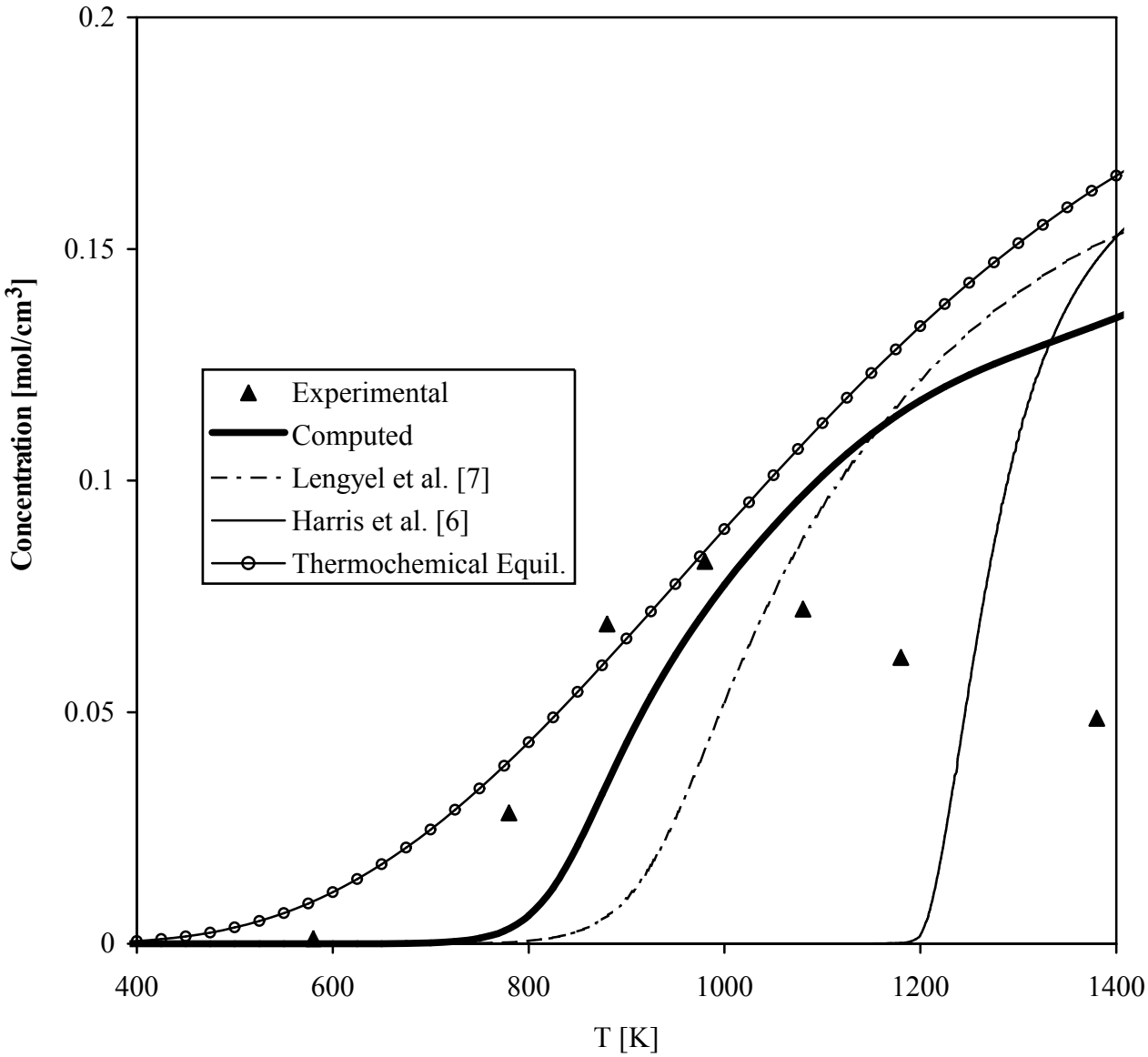
0.2
0.15
0.1
0.05
0
Concentration [mol/cm3]
400
600
800
1000
1200
1400
T [K]
Experimental
Computed
Lengyel et al. [7]
Harris et al. [6]
Thermochemical Equil.